

This article was downloaded by: [Tomsk State University of Control Systems and Radio]

On: 23 February 2013, At: 03:08

Publisher: Taylor & Francis

Informa Ltd Registered in England and Wales Registered Number: 1072954

Registered office: Mortimer House, 37-41 Mortimer Street, London W1T 3JH, UK



Molecular Crystals and Liquid Crystals

Publication details, including instructions for authors and subscription information:

<http://www.tandfonline.com/loi/gmcl16>

Liquid Crystal Cross-Pattern Display Characteristics

F. Ogawa^a, S. Naemura^a & C. Tani^a

^a Central Research Laboratories, Nippon Electric Co., Ltd., 4-1-1, Miyazaki, Takatsuku, Kawasaki, 213, Japan

Version of record first published: 14 Oct 2011.

To cite this article: F. Ogawa, S. Naemura & C. Tani (1981): Liquid Crystal Cross-Pattern Display Characteristics, *Molecular Crystals and Liquid Crystals*, 70:1, 251-266

To link to this article: <http://dx.doi.org/10.1080/00268948108073592>

PLEASE SCROLL DOWN FOR ARTICLE

Full terms and conditions of use: <http://www.tandfonline.com/page/terms-and-conditions>

This article may be used for research, teaching, and private study purposes. Any substantial or systematic reproduction, redistribution, reselling, loan, sub-licensing, systematic supply, or distribution in any form to anyone is expressly forbidden.

The publisher does not give any warranty express or implied or make any representation that the contents will be complete or accurate or up to date. The accuracy of any instructions, formulae, and drug doses should be independently verified with primary sources. The publisher shall not be liable for any loss, actions, claims, proceedings, demand, or costs or damages

whatsoever or howsoever caused arising directly or indirectly in connection with or arising out of the use of this material.

Liquid Crystal Cross-Pattern Display Characteristics†

F. OGAWA, S. NAEMURA and C. TANI

*Central Research Laboratories, Nippon Electric Co., Ltd.
4-1-1, Miyazaki, Takatsuku, Kawasaki 213 Japan*

(Received August 1, 1980; in final form November 5, 1980)

This paper presents characteristics of a prototype liquid crystal cross-pattern display utilizing a cholesteric nematic phase transition mode. Dielectrically positive cholesteric liquid crystal material used is a mixture of biphenyl nematic and cholesteric nonanoate in 9:1 weight ratio. In order to display a cross-pattern, four different signals made from phase shifted do-rectangular waveforms are applied to striped row and column electrodes. Display rise time and fall time are typically 30 msec. and 100 msec., respectively, which enable fast cross-pattern display scanning.

INTRODUCTION

Among the various operating modes utilized in liquid crystal displays (LCDs), the cholesteric-nematic phase transition (CNPT) mode generally has the following features: (1) The acceptable viewing angle is larger than 140° . (2) Display response speed is fast. (3) The restriction on temperature and humidity surrounding LCDs can be relaxed by eliminating polarizer. In particular, several matrix character displays, utilizing the CNPT mode have been developed.¹⁻³

This paper presents characteristics of a prototype liquid crystal cross-pattern display⁴ developed by utilizing the CNPT mode, for other applications than for a character display. This display can indicate the position of an object by overlaying the cross-pattern on or under a certain fixed figure. Striped electrodes on the two glass plates with homeotropic boundary condition are in a matrix format.

†Presented at the Eighth International Liquid Crystal Conference in Kyoto, June 30-July 4, 1980.

PRINCIPLE

Dielectrically positive cholesteric liquid crystal (LC) cells with homeotropic boundary conditions in its quiescent state exhibits an almost transparent spiral state S (Cholesteric Phase).¹ It changes to a scattering fan-shaped state F (Cholesteric Phase) on voltage application, and transforms at threshold voltage V_H to a homeotropic nematic state H (Nematic Phase) as a result of the field-induced CNPT.

When the voltage applied to the LC cell is changed from V_2 to V_1 ($V_2 < V_H < V_1$), the cell changes from state F to state H . But, when the voltage applied to the LC cell is changed from V_1 to V_2 ($0.3 V_H < V_2 < V_H$), a metastable homeotropic state H' is maintained for a rather long time T , that depends on V_2/V_H . In order to obtain the rapid transition from state H to state F' , where state F' is the strong scattering focal-conic state, the voltage applied to the LC cell should be changed from V_1 to zero, and after t_0 msec. ($t_0 \geq \tau_{NC}$, where τ_{NC} is the nematic-cholesteric phase relaxation time), zero to V_2 . State F' is transitioned to state F , slowly.

DRIVING SCHEME

In order to display a cross-pattern by using one row (i) and one column (j), and form the background by using other rows (k) and other columns (l), four different signals, $Q(0)$, $Q(\pi)$, $Q(-\pi)$ and $Q(\pi - \theta)$, are made from phase shifted dc-rectangular waveforms (frequency $f = 1/2t$, voltage height V_{op}), and applied to row and column electrodes, (Figure 1). π , $-\theta$ and $(\pi - \theta)$ mean the phase differences from the signal $Q(0)$. The ac-rectangular waveform ($S1$) signal with duty ratio $D = \theta/\pi$, which is made from the combination of $Q(0)$ and $Q(-\theta)$, or $Q(\pi)$ and $Q(\pi - \theta)$, is applied to selected dots, which form a cross-pattern having light scattering state F' or F , during the selected period except for time interval t_0 at the time of the transition from state H to state F' . Another signal ($S2$) with $D = 1$, which is made from the combination of $Q(0)$ and $Q(\pi)$, or $Q(-\theta)$ and $Q(\pi - \theta)$, is applied to non-selected dots, which form the background in transparent homeotropic nematic state H . Voltage heights for $S1$ and $S2$ are the same value V_{op} . The rms voltages, V_{rms} , for $S1$ and $S2$ are $(\theta/\pi)^{1/2} V_{op}$ and V_{op} , respectively. θ and V_{op} should satisfy inequalities, $1/3 V_H' < (\theta/\pi)^{1/2} V_{op} < V_H$ and $V_{op} > V_H$, where V_H' and V_H are threshold rms voltage for cholesteric-nematic phase induced by $S1$ and $S2$, respectively. $S1$ and $S2$ are shown in Figure 2. When the duty ratio for applied signal to the dots changes from 1 to 0 and, after t_0 msec., 0 to θ/π , the rms voltage for applied signal is changed from V_{op} to zero and, after t_0 msec., zero to $(\theta/\pi)^{1/2} V_{op}$, as shown in Figure 3. The dots are changed from non-selected dots in state H to selected dots in state F' , rapidly, by the signal change.

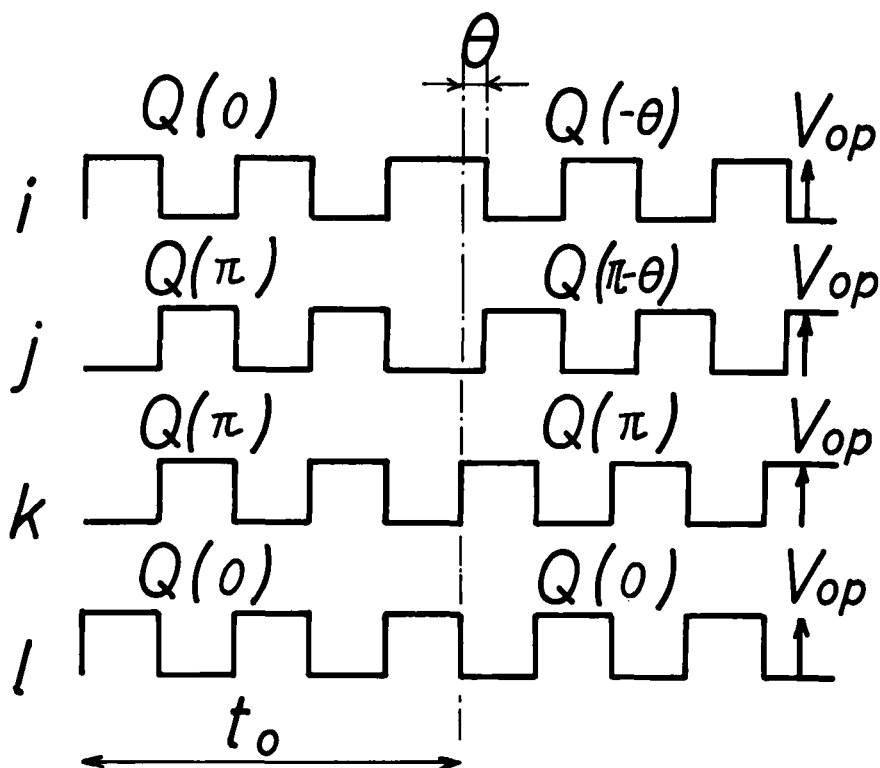


FIGURE 1 Phase shifted dc-rectangular waveforms applied to selected row (i) and column (j) electrodes, and to non-selected row (k) and column (l) electrodes π , $-\theta$ and $(\pi - \theta)$; phase differences from the signal $Q(0)$.

The driving method mentioned above needs only two voltage levels (0 and V_{op}). This leads to a driving circuit simplicity merit.

LIQUID CRYSTAL MATERIALS

The LC materials used for the present LCD are dielectrically positive mixtures of nematics and cholesterics. Desired LC material characteristics are a small τ_{NC} (≤ 30 rms) and a low V_H , compatible with C-MOS driving circuits, throughout the operating temperature range required by the LC itself only, 20–70°C. Various LC mixtures were sought with large dielectric anisotropy $\Delta\epsilon$ (> 0) and small viscosity η to satisfy the demands. Finally, a mixture of biphenyl nematics and a cholesteryl ester was selected. The cholesteric concentration was selected to be 10 wt. % to realize the LC quiescent pitch $P_0 = 1.9 \mu\text{m}$, which is the optimum value for small τ_{NC} and V_H . This mixture has a clearing temperature of 96°C and shows the cholesteric phase even at

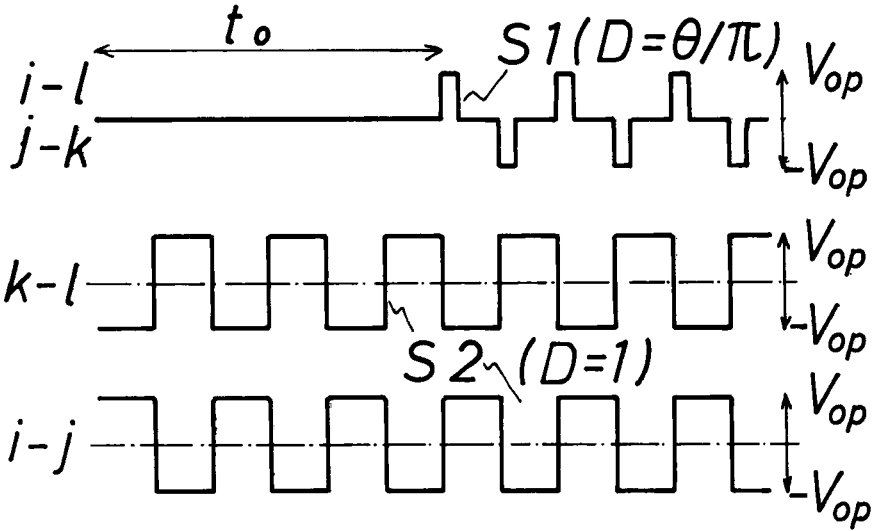


FIGURE 2 Ac-rectangular waveforms applied to selected and non-selected dots. S_1 , duty ratio $= \theta/\pi$; S_2 , duty ratio $= 1$.

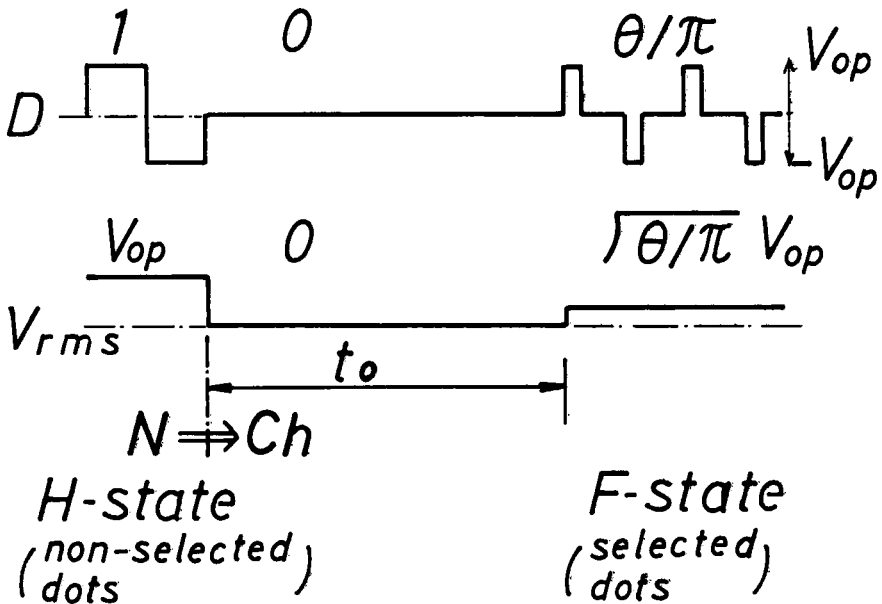
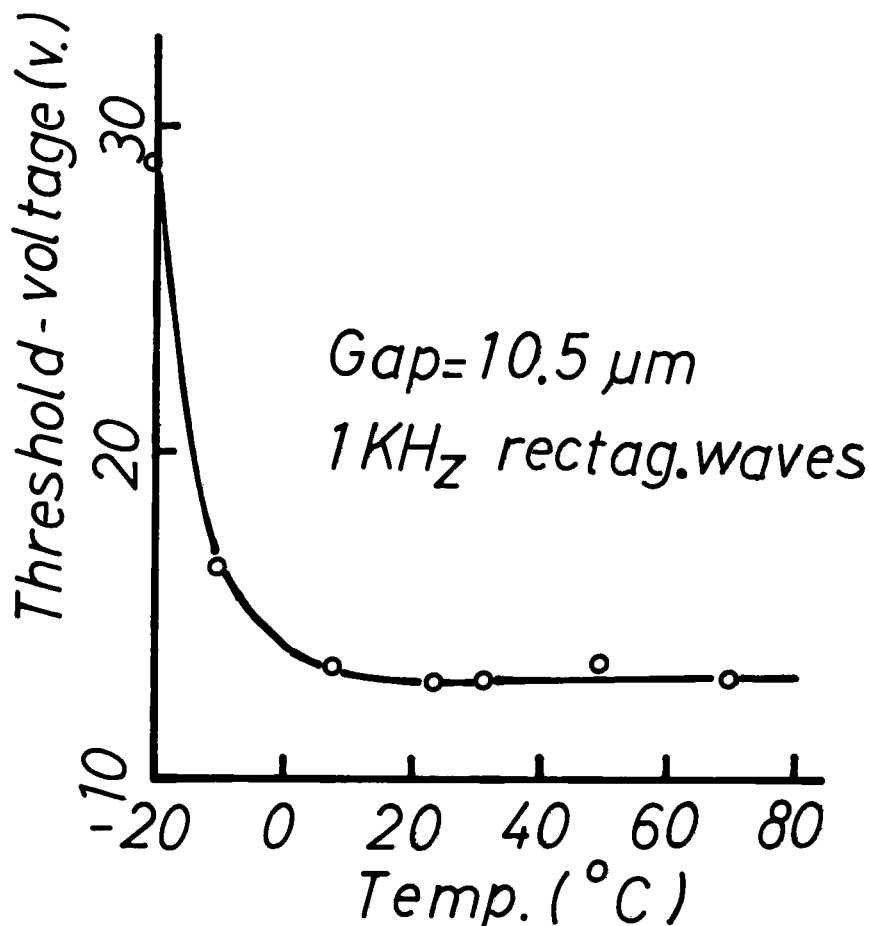


FIGURE 3 The relation of duty ratio and rms voltage for applied signal to dots which are changed from non-selected dots to selected dots.

FIGURE 4 Threshold voltage V_H temperature dependence.

-20°C for over 6 hours. V_H shows an extremely small temperature dependence above 10°C and is 13 volts for $10.5\ \mu\text{m}$ layer thickness (Figure 4). τ_{NC} and τ_{CN} temperature dependence are shown in Figure 5. Above 20°C , we can obtain $\tau_{NC} \leq 25\ \text{ms.}$ and $\tau_{CN} = 100\ \text{ms.}$ ($V = 2 V_H$). Thus, this LC material was found to be adoptable for present use.

CHARACTERISTICS

Light transmission characteristics were measured by using the ac-rectangular waveform signals mentioned in the driving scheme section. Measurements were performed using He-Ne laser. Light transmission vs. applied rms vol-

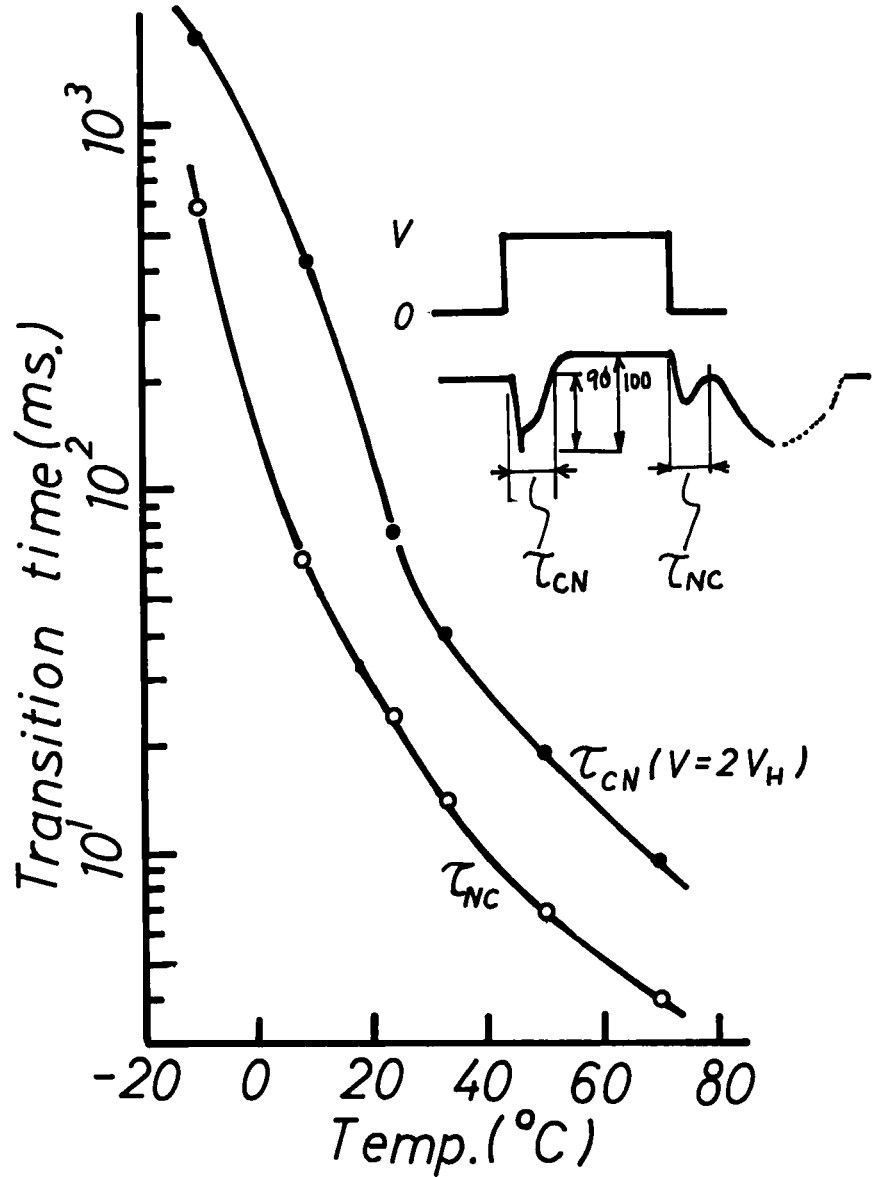


FIGURE 5 Transition times τ_{NC} and τ_{CN} temperature dependence.

tages curves depend on the duty ratio for ac-rectangular waveforms, as shown in Figure 6 when frequency f for the applied voltage is low, for example 50 Hz. Threshold rms volate V'_H increases with decreasing duty ratio D . Minimum and maximum driving voltages are $V_H = 10$ V. ($D = 1$) and $(1/D)^{1/2} \cdot V'_c = 19$ V. ($D = 1/3$), 21 V. ($D = 1/4$), 41 V. ($D = 1/10$), respectively. Figure 6

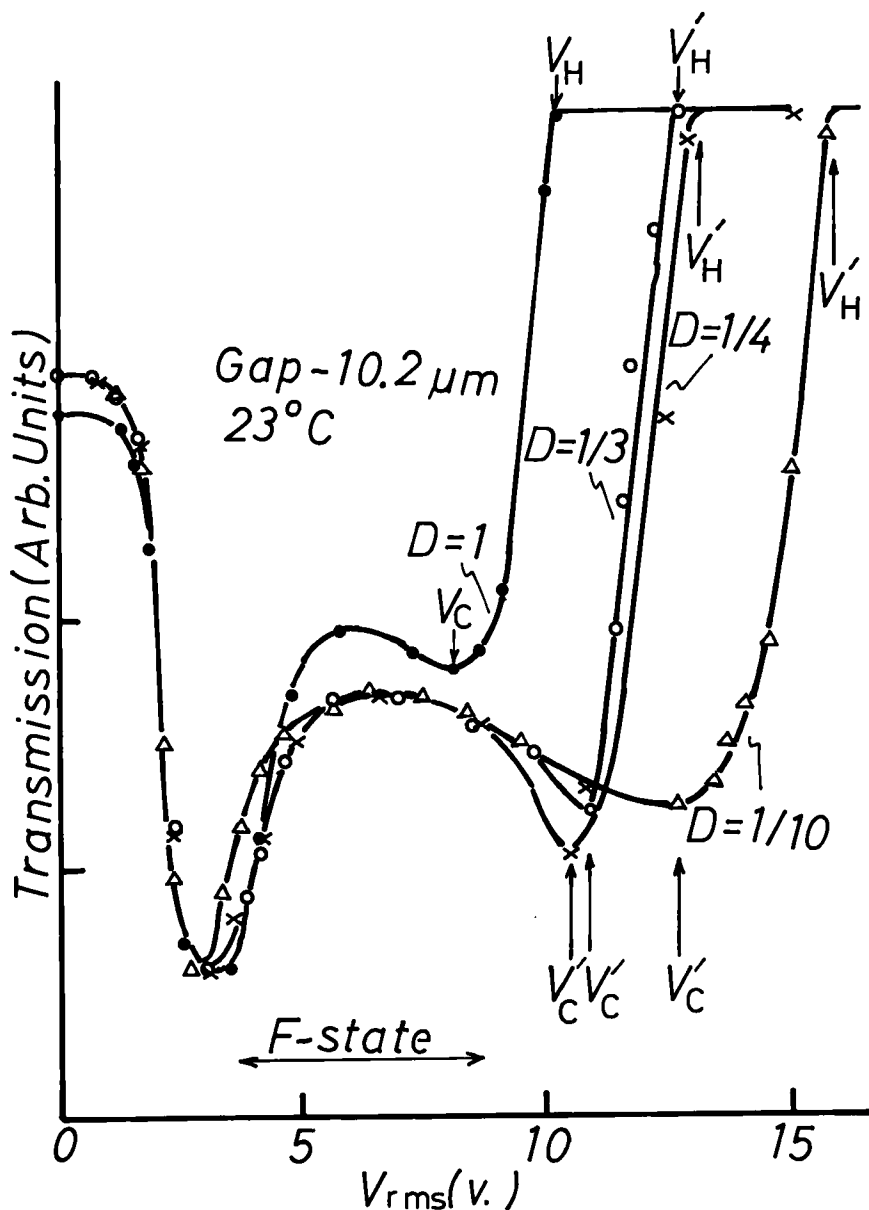


FIGURE 6 Light transmission vs. applied rms voltages curves.

shows that transmission intensities for curve $D = 1$ in the F state are lower than for curve $D = 1$. This is caused by the fluctuation in transmission, as shown in Figure 7. The fluctuation peak level shown in Figure 6 corresponds to the transmission level for curve $D = 1$ in F state.

When the duty ratio for an applied signal is changed from θ/π to 1, the rms

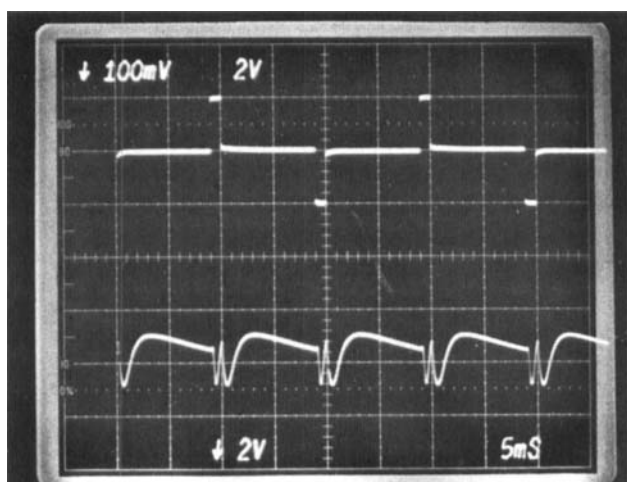


FIGURE 7 Light transmission fluctuation in *F*-state (duty ratio = 1/10, $V_{op} = 20$ V, $f = 50$ Hz).

voltage changes from $(\theta/\pi)^{1/2} V_{op}$ to V_{op} , and cholesteric-nematic phase transition occurs (see Figure 8: $V_{op} = 16$ v, $D = 1/4 \rightarrow 1$, $f = 50$ Hz).

Transition time t_{CN} (display fall time) is independent from duty ratio for applied signals to keep state *F* and is approximately inversely proportional to V_{op}^2 , as shown in Figure 9. On the other hand, when duty ratio for applied signal is changed from 1 to 0 and, after t_0 msec., 0 to θ/π , the rms voltage

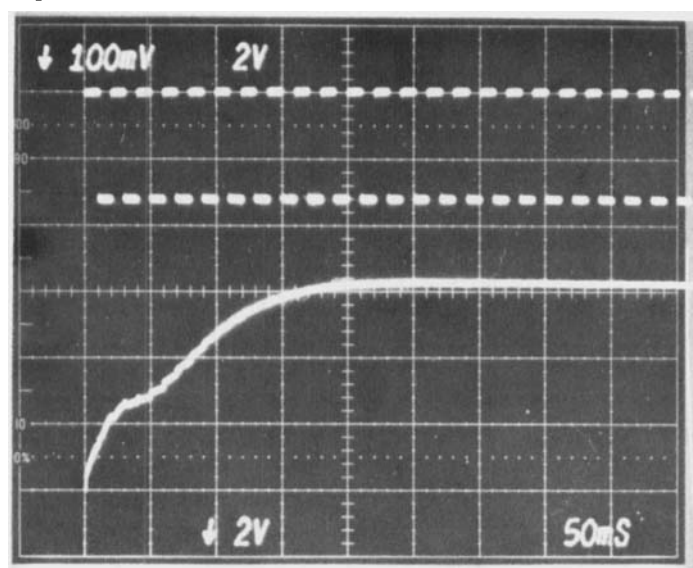


FIGURE 8 Cholesteric-nematic phase transition characteristics ($V_{op} = 16$ V, $D = 1/4 \rightarrow 1$, $f = 50$ Hz).

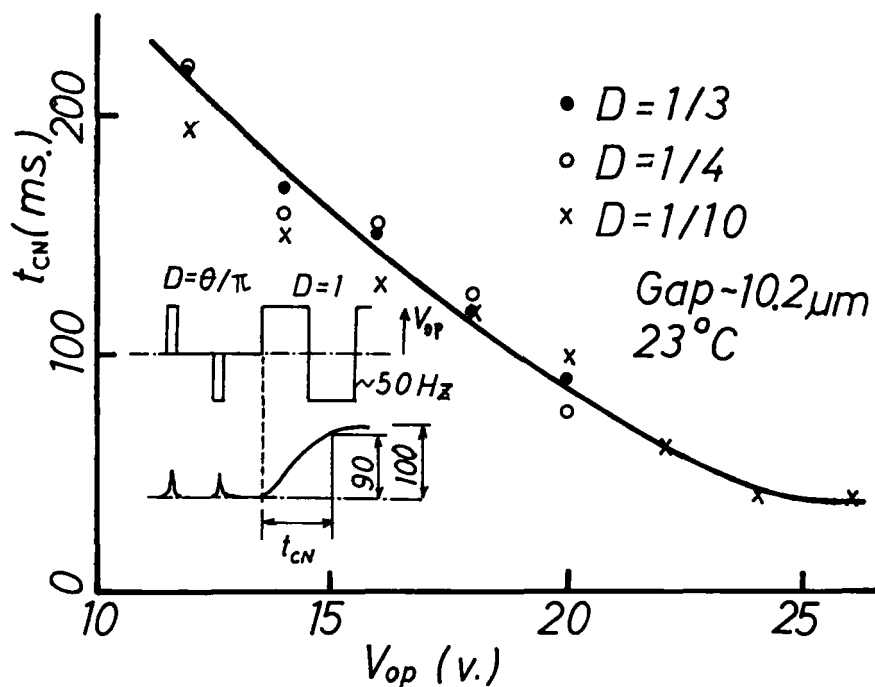
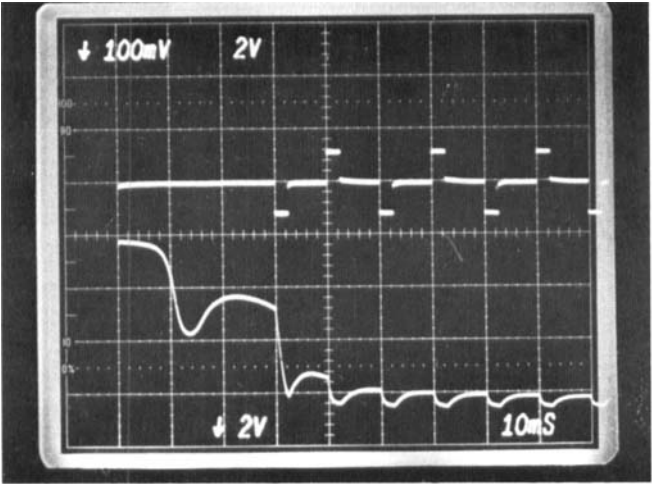
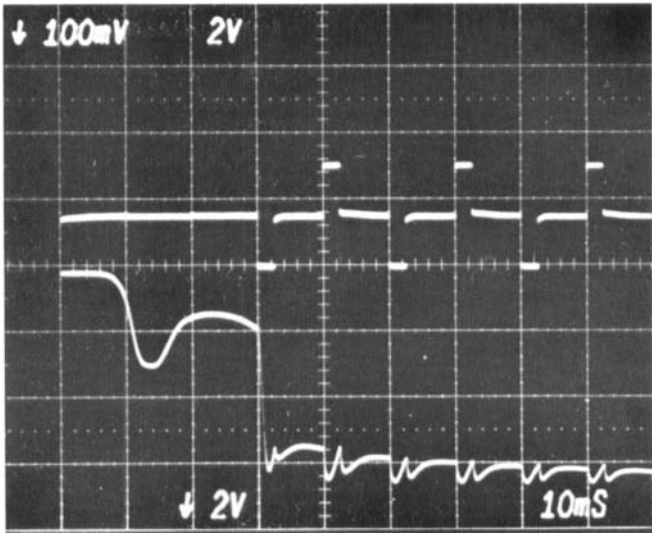


FIGURE 9 Cholesteric-nematic phase transition time, t_{NC} , vs. driving voltage, V_{op} ($t_{NC} \propto V_{op}^{-2}$).

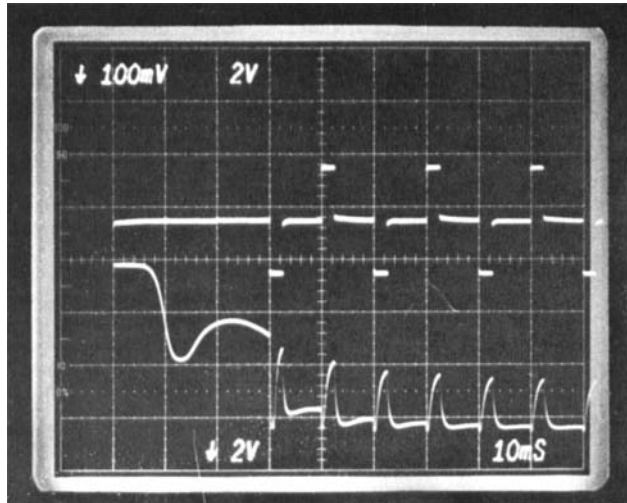
changes from V_{op} to 0 and, after t_0 msec., 0 to $(\theta/\pi)^{1/2} V_{op}$ and nematic-cholesteric phase transition occurs. Transition time t_{NC} (display rise time) is approximately equal to t_0 . t_0 should be slightly longer than or equal to τ_{NC} , which is nematic-cholesteric phase relaxation time. Nematic-cholesteric phase transition characteristics under $V_{op} = 12 \text{ V}$, 15 V and 20 V applied voltages are shown in Figures 10(a), (b) and (c), respectively, when the duty ratio for an applied signal is changed as follows; $D = 1 \rightarrow 0$ (30 msec) $\rightarrow 1/4$. The characteristic in Figure 10(b) is better than the others. When the duty ratio for applied voltage is changed as follows; $D = 1 \rightarrow 0$ (30 msec) $\rightarrow 1/10$, the better nematic-cholesteric phase transition characteristic is obtained under the applied voltage $V_{op} = 22 \text{ V}$ (see Figure 11). $V_{op} = 15 \text{ V}$ [Figure 10(b)] and $V_{op} = 22 \text{ V}$ (Figure 11) correspond to rms voltages, $V_{rms} = 7.5 \text{ V}$ and 7 V , respectively, which are the rms voltages for the transmission peak levels in F -state in Figure 6. When the duty ratio for the applied signal is changed from 1 to θ/π , transition time, t_{NC} , becomes much longer than the nematic-cholesteric phase relaxation time τ_{NC} (see Figure 12; $D = 1 \rightarrow 1/10$, $V_{rms} = 16 \text{ V} \rightarrow 3.2 \text{ V}$), and is shortened with decreasing $V_{rms} = D^{1/2} V_{op}$.¹ When the voltage height is changed as follows: $V_1 (= 16 \text{ V} > V_H) \rightarrow 0$ (30 msec) $\rightarrow V_2 (8 \text{ V} < V_H)$, when $f = 1 \text{ kHz}$ and duty ratio = 1, transition time, t_{NC} , becomes



(a)



(b)



(c)

FIGURE 10 Nematic-cholesteric phase transition characteristics (duty ratio, $1 \rightarrow 0$ (30 msec) $1/4$, $f = 50$ Hz); (a) $V_{op} = 12$ V, (b) $V_{op} = 15$ V, (c) $V_{op} = 20$ V.

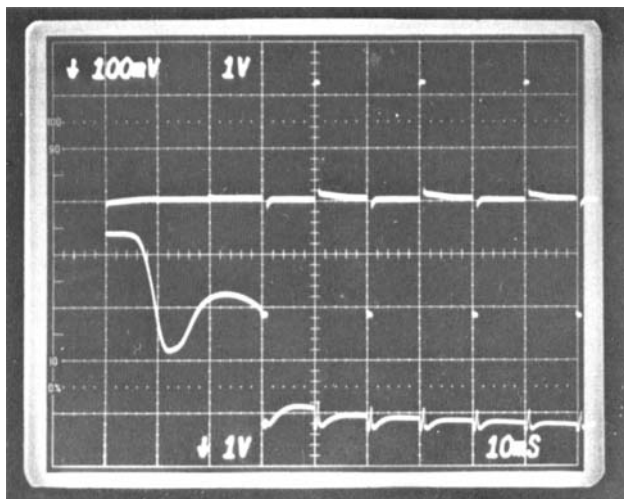


FIGURE 11 Nematic-cholesteric phase transition characteristics $V_{op} = 22$ V, duty ratio; $1 \rightarrow 0$ (30 msec) $\rightarrow 1/10$, $f = 50$ Hz.

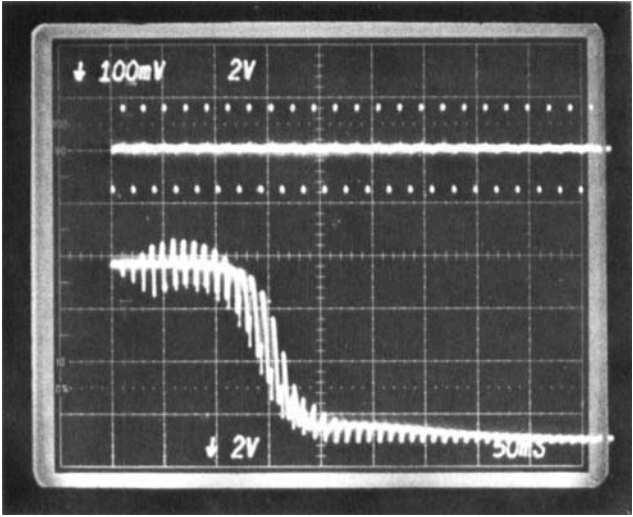


FIGURE 12 Nematic-cholesteric phase transition characteristics $V_{op} = 16$ V, duty ratio; $1 \rightarrow 1/10$, $f = 50$ Hz.

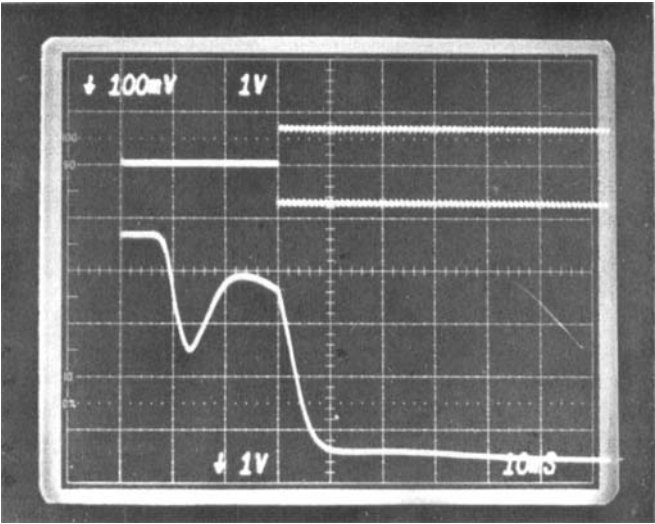


FIGURE 13 Nematic-cholesteric phase transition characteristics V_{op} ; 16 V $\rightarrow 0$ (30 msec) $\rightarrow 8$ V. $D = 1$ $f = 1$ kHz.

longer than 30 msec (see Figure 13). So, the nematic cholesteric phase transition time, t_{NC} , can be shortened by the driving scheme shown in Figure 3.

Table I shows typical cross-pattern display performance.

CROSS-PATTERN DISPLAY TEMPERATURE DEPENDENCE

The cross-pattern display was observed through a window in the cooling and heating box under the following conditions. Temperature range is from -40°C to 90°C , $V_{op} = 15\text{ V}$, $t_0 = 30\text{ msec}$, $D = 1$ and $1/4$, $f = 50\text{ Hz}$. The display contrast is deteriorated below 20°C and the cross-pattern does not appear below 10°C , because the nematic-cholesteric phase relaxation takes longer time than $t_0 = 30\text{ msec}$ below 20°C (see Figure 5) and the display rise time becomes longer than the cross-pattern scanning time/line. The cross-pattern can be observed to be excellent between 20°C and 70°C . The display contrast is deteriorated at higher temperature than 70°C , because the transmission fluctuation amplitude caused by voltage on-off cycle for duty ratio $D < 1$ increases with decreasing cholesteric-nematic phase transition time at high temperature (see in Figure 5). The display contrast can be improved by using higher frequency signals at higher temperature.

TABLE I

Typical cross-pattern display performance

V_{op}	D	t_0	t_{CN}	t_{NC}	$v = 1/t_{CN}$
15 v.	1/4	30 _{ms.}	165 _{ms.}	30 _{ms.}	6 _{lines/s.}
22 v.	1/10	30 _{ms.}	65 _{ms.}	30 _{ms.}	15 _{lines/s.}

v : moving speed of
cross-pattern

TABLE II

Panel shape

<i>Panel Size</i>	$63 \times 63 \times 4.8 \text{ mm}^3$
<i>Display Area</i>	$46 \times 46 \text{ mm}^2$
<i>Number of Electrodes</i>	40×40
<i>Resolution</i>	1 dot/mm
<i>Dot Size</i>	$0.9 \times 0.9 \text{ mm}^2$
<i>LC Layer Thickness</i>	$8.5 \pm 0.7 \text{ }\mu\text{m}$

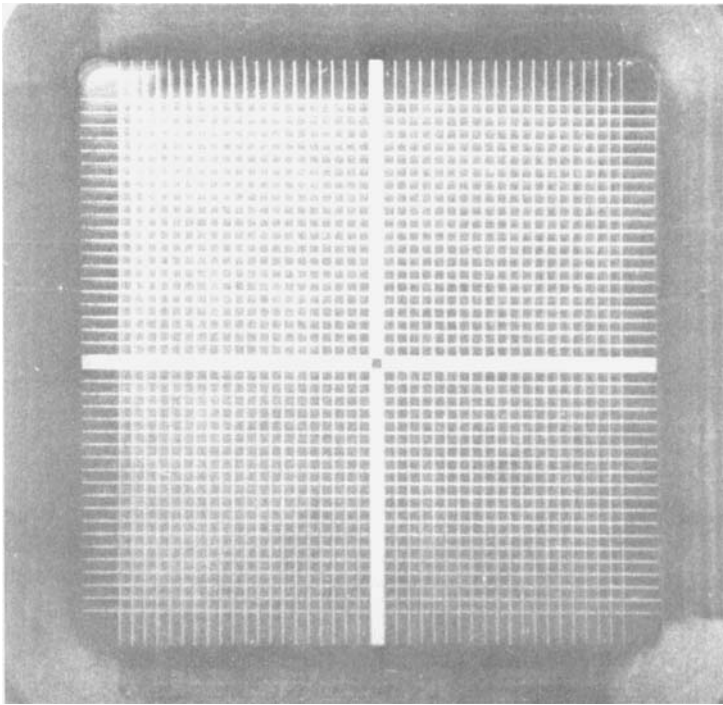


FIGURE 14 Cross-pattern display.

TABLE III

Electrical performance

<i>Driving Voltage 12 ~ 18 v.</i> <i>(C - MOS ICs)</i> $D = 1/4$ $t_o = 30 \text{ ms.}$ $f = 50 \text{ Hz}$
<i>Heater 10 w (160Ω)</i> <i>4 min. (- 25 \rightarrow 25 $^{\circ}$C)</i>
<i>Operarating Temp.</i> <i>20 ~ 70$^{\circ}$C (-25-70$^{\circ}$ C</i> <i>with heater)</i>
<i>Moving Speed of</i> <i>Cross Pattern</i> 5 l./s. (12 v.) 6 l./s. (15 v.) 10 l./s. (18 v.)

CONCLUSION

This paper has described a driving scheme and characteristics of the cross-pattern display using the cholesteric nematic phase transition mode. The driving scheme needs only two voltage levels (0 and V_{op}). This leads to driving circuit simplicity. Moreover, one can use C-MOS ICs because of the low threshold voltage ($\sim 10 \text{ V}$). The display rise time is approximately equal to the nematic-cholesteric relaxation time, which depends on the helical pitch length of liquid crystal material. It is usually a few tens of milliseconds or shorter.

This display can be operated in a wide temperature range ($-25^{\circ}\text{C} \sim 90^{\circ}\text{C}$) with a heater and a temperature compensation circuit to make signal frequency higher at higher temperature. This display using the bihenyle-nematics and cholesteric mixture, the organic surfactant for homeotropic alignment and plastic sealing material, underwent reliable tests, kept for 8 hours at -40°C and cycling the temperature and humidity, as follows; room temperature $\rightarrow 38^{\circ}\text{C}$ 85% RH $\xrightarrow{2\text{ hrs.}}$ 71°C 95% RH keeping for 6 hrs. $\xrightarrow{2\text{ hrs.}}$ 38°C 85% RH \rightarrow room temperature (naturally cooling), 3 cycles/3 days. Thus, this display has a wide storage temperature range ($-40^{\circ}\text{C} \sim 90^{\circ}\text{C}$) and environment reliability. This display also has a wide viewing angle ($> 140^{\circ}$) and does not need a polarizer.

Table II shows the panel shape and Table III shows electrical performance. This liquid crystal cross-pattern display, (shown in Figure 14), has a capability of adapting as a position control monitor, such as an airplane instrument.

Acknowledgments

The authors wish to extend their appreciation to Dr. F. Saito for encouragement and invaluable advice. The authors also wish to thank Mr. T. Ueno for his helpful discussions. The authors also wish to thank Mr. M. Kajiyama, Mr. S. Shiraishi, Mr. K. Kobayashi and Mr. Y. Takizawa for their helpful cooperation in the course of this work.

References

1. C. Tani, F. Ogawa, S. Naemura, T. Ueno, F. Saito and O. Kogure, *Proceed. S.I.D.*, **21**, 71 (1980).
2. T. Ohtsuka, M. Tsukamoto and M. Tsuchiya, *Japan J.A.P.*, **12**, 371 (1973).
3. K. H. Walter and M. K. Tauer, *IEEE Trans. E.D.*, **ED25**, 172 (1978).
4. R. P. Farnsworth, L. W. Hill and S. Y. Wong, U.S. Patent No. 3885861 May 27 (1975).